MATHEMATICAL ENGINEERING
TECHNICAL REPORTS

Exploring New Tensegrity Structures via Mixed Integer Programming

Yoshihiro KANNO

METR 2012–17 October 2012

DEPARTMENT OF MATHEMATICAL INFORMATICS
GRADUATE SCHOOL OF INFORMATION SCIENCE AND TECHNOLOGY
THE UNIVERSITY OF TOKYO
BUNKYO-KU, TOKYO 113-8656, JAPAN

WWW page: http://www.keisu.t.u-tokyo.ac.jp/research/techrep/index.html

Exploring New Tensegrity Structures via Mixed Integer Programming

Yoshihiro Kanno †

Department of Mathematical Informatics,
University of Tokyo, Tokyo 113-8656, Japan

Abstract

A tensegrity structure is a prestressed pin-jointed structure consisting of continuously connected tensile members (cables) and disjoint compressive members (struts). Many classical tensegrity structures are prestress stable, i.e., they are kinematically indeterminate but stabilized by introducing prestresses. This paper presents a procedure for generating various prestress stable tensegrity structures. This method is based on truss topology optimization and does not require connectivity relation of cables and struts of a tensegrity structure to be known in advance. The optimization problem with the constraints expressing the definition of tensegrity structure, kinematical indeterminacy, and symmetry of configurations is formulated as a mixed integer linear programming (MILP) problem. Numerical experiments demonstrate that various tensegrity structures can be generated from a given initial structure by solving the presented MILP problems with varying some parameters.

Keywords

Tensegrity; Prestressed structure; Topology optimization; Integer programming; Symmetry.

1 Introduction

A *tensegrity structure* is a free-standing prestressed pin-jointed structure consisting of a set of discontinuous compressive components (struts) interacting with a set of continuous tensile components (cables) [26]. Most of classical tensegrity structures in literature are kinematically indeterminate [4, 13, 14, 27]. Those tensegrity structures are, therefore, unstable without prestress but are stabilized by introducing prestress. Such a structure is said to be *prestress stable* [8].

The discontinuity condition of struts is an intrinsically difficult constraint in designing tensegrity structures. Therefore, in most of existing design methods, connectivity of cables and struts, i.e., topology, of a tensegrity structure is required to be specified as input data; see surveys due to Juan and Mirats Tur [17] and Tibert and Pellegrino [37] for various form-finding methods of tensegrity structures.

†Address: Department of Mathematical Informatics, Graduate School of Information Science and Technology, University of Tokyo, Tokyo 113-8656, Japan. E-mail: kanno@mist.i.u-tokyo.ac.jp. Phone: +81-3-5841-6906, Fax: +81-3-5841-6886.

For exploring new tensegrity structures, however, specification of topology might possibly be too restrictive. As methods requiring no information of topology in advance, the author proposed mixed integer programming approaches to compliance optimization of tensegrity structures under a given external load [19] and a self-weight load [18]. Almost all tensegrity structures obtained by these methods are kinematically determinate, although constraints on stability were not considered in [18, 19]. In contrast, as mentioned before, many well-known tensegrity structures in literature are kinematically indeterminate and prestress stable [4, 13, 14, 27, 42, 43]. Prestress stability is not only interesting as a research subject of structural engineering but also considered a resource of artistic excellent impression of these tensegrity structures; indeed, many tensegrity structures in the real world are realized as fascinating sculptures by artists [15] and as distinctive architectural structures [3]. The motivation of this paper, therefore, is to develop a method that can find prestress stable tensegrity structures. In continuation of the previous works [18, 19], we employ discrete topology optimization of trusses based upon the ground structure method to find tensegrity structures. A *mixed integer linear programming* (MILP) approach is used to solve the structural optimization problem.

To find tensegrity structures with kinematical indeterminacy, we introduce a constraint on the numbers of struts and cables based upon the Maxwell counting rule for rigidity [6]. The optimization problem that we solve does not attempt to improve mechanical performance, because it was demonstrated in [18, 19] that improvement of compliance usually yields kinematically determinate solutions. Note that in this paper we do not discuss whether prestress stability has some advantage in mechanical performances over usual stability; exploring kinematically indeterminate structures is probably unreasonable from a view point of designing structures with high mechanical performance. Moreover, in this paper we assume small deformations and do not consider any constraints involving geometrical nonlinearity. Therefore, the proposed method is not guaranteed to generate tensegrity structures that are stabilized by introducing prestress forces. Nonetheless, solutions obtained by the method are often prestress stable as demonstrated by numerical examples in section 6.

Many studies have been made on finding tensegrity structures with high symmetry in configurations, because most of tensegrity structures that have long been known have symmetric configurations. Particularly, advanced techniques for generating topologies of tensegrity structures that enjoy the same group symmetry have been developed in [5, 7, 24]. In contrast, there exist a few numerical methods that are not limited to symmetric tensegrity structures. Some of those methods are basically find asymmetric configurations by modifying a given symmetric tensegrity structure [2, 25, 38, 44]. Recent interest has been drawn for developing versatile numerical methods that require no information of existing tensegrity structures as input data and can generate diverse non-symmetric tensegrity structures. To this end, optimization problems involving discrete variables were solved with evolutionary algorithms [30, 41] and MILP approaches [18, 19]. Li *et al.* [22] proposed to employ the Monte Carlo simulation. Li *et al.* [23] developed a systematic method to construct a tensegrity structure by connecting some elementary cells, each of which consists of one strut and a few cables. Tran and Lee [38] proposed a method based on the singular value decomposition of the equilibrium matrix, where an initial force-density vector is randomly generated.

In this paper we introduce the constraint on the number of different member lengths to achieve diversity of symmetry properties of tensegrity structures generated by the proposed method. As this number increases, symmetry of a structure becomes lower. Conversely, a structure with high symmetry has small number of different member lengths. Therefore, by varying the number of different member lengths we can generate tensegrity structures with various symmetry properties from a given ground structure. In other words, symmetry of solutions is implicitly controlled by this number. Symmetry of optimal structure of convex and nonconvex optimization problems has received increasing attention recently; see, e.g., [1, 11, 21, 32, 35, 40]. Since the optimization problem solved in the proposed method is nonconvex, the optimal solution is not symmetric in general even if input data is given to be symmetric. By specifying a small number of different member lengths, symmetry of the optimal solution becomes as high as possible. In contrast, if the number of different member lengths is specified to be large, e.g., if it is equal to the number of existing members, then the optimal solution is guaranteed to have no symmetry.

All of the constraints above are treated within the framework of MILP. Therefore, the global optimal solution can be found by using, e.g., a branch-and-cut algorithm. MILP approaches were applied to topology optimization of continua [36] and trusses [20, 29].

The paper is organized as follows. Section 2 presents a definition of tensegrity structures that we adopt in this paper. The basic idea for formulating MILP problems for tensegrity optimization in [18, 19] is also recalled briefly. Section 3 introduces the constraint on the number of different member lengths, which implicitly controls symmetry of structures. In section 4, we formulate the constraint ensuring kinematical indeterminacy based upon the Maxwell counting rule and propose a procedure for generating various tensegrity structures from a given ground structure. In section 5, we formulate an MILP problem that is solved for finding tensegrity structures. Three numerical examples are demonstrated in section 6. We conclude in section 7. The detail of MILP formulation is presented in appendix A.

2 Preliminary results

We formulate the constraints representing a definition of tensegrity structure as linear equality and linear inequality constraints in terms of continuous variables and integer variables. Then an MILP problem involving those constraints is solved to find a new tensegrity structure. An essential idea for this methodology, presented in [18, 19], is to make use of integer variables serving as labels of members. In this section we summarize fundamental constraints on a tensegrity structure. The notion of a member label is also briefly recalled to make this paper self-contained. The constraints regarding symmetry and kinematical indeterminacy will be addressed in section 3 and section 4, respectively.

2.1 Constraints on tensegrity condition

Like the conventional ground structure method for truss topology optimization, we prepare an initial pin-jointed structure consisting of sufficiently many candidate members. Locations of the nodes of the initial structure are specified in the three-dimensional space. We use V and E to

denote the set of nodes and the set of members, respectively. Note that a tensegrity structure is a free-standing prestressed structure. Therefore, the initial structure has no fixed support and the number of degrees of freedom of displacements is $3|V|$, where $|V|$ denotes the cardinality of V.

As mentioned in section 1, attention of this paper is focused on finding tensegrity structures that are kinematically indeterminate. More specifically, in this paper, a free-standing kinematically indeterminate cable–strut structure is said to be a tensegrity structure if it has a unique state of self-stress satisfying the following conditions:

(i) Each member transmits either a nonzero compression force or a nonzero tension force.

(ii) Each node is connected to exactly one compressive member.

(iii) The structure is stabilized by introducing the self-equilibrium forces.

The self-equilibrium forces satisfying these conditions can be introduced as *prestress forces*. Regarding condition (i), we call a member transmitting a compression force a *strut* and a member transmitting a tension force a *cable*. Condition (ii) is called the *discontinuity condition of struts*, i.e., struts should not touch each other. Condition (iii) means that the tangent stiffness matrix in the presence of prestress forces is positive definite. A tensegrity structure satisfying this condition is said to be *prestress stable*; see [8, 10] for more details of prestress stability. Besides these three conditions, we shall consider some additional constraints that are naturally required from a practical point of view.

There exist various definitions of tensegrity [26]. For instance, Skelton and de Oliveira [34] introduced the notion of class-k tensegrity structure, where k is the maximum number of struts that touch each other. Within this terminology, a tensegrity structure satisfying condition (ii) is a class-1 tensegrity. Thus the discontinuous condition of struts is sometimes relaxed in literature. In the author's previous work [18, 19], kinematical indeterminacy, prestress stability, and uniqueness of self-equilibrium mode of axial forces were not considered.

Let $\boldsymbol{q} = (q_i) \in \mathbb{R}^{|E|}$ denote the vector of axial forces introduced to the members as prestress forces. We next formulate some constraints that $\boldsymbol{q}$ should satisfy. Since $\boldsymbol{q}$ is the vector of self-equilibrium forces, it satisfies the static equilibrium equation without external forces. This condition is written as

$$H\boldsymbol{q} = \boldsymbol{0}, \tag{1}$$

where $H \in \mathbb{R}^{3|V|\times|E|}$ is the equilibrium matrix.

Note that we remove some members from the initial structure to obtain a tensegrity structure. Let $\{S, C, N\}$ be a partition of E, where S, C, and N are the sets of struts, cables, and removed members, respectively. Condition (i) means that $q_i < 0$ $(\forall i \in S)$, $q_i > 0$ $(\forall i \in C)$, and $q_i = 0$ $(\forall i \in N)$. In conjunction with practical lower and upper bounds for prestress forces, the constraints on q_i are given by

$$q_i \in \begin{cases} [-\overline{q}^{\mathrm{s}}, -\underline{q}^{\mathrm{s}}] & \text{if } i \in S, \\ [\underline{q}^{\mathrm{c}}, \overline{q}^{\mathrm{c}}] & \text{if } i \in C, \\ \{0\} & \text{if } i \in N, \end{cases} \tag{2}$$

where $\underline{q}^{\mathrm{s}}$, $\overline{q}^{\mathrm{s}}$, $\underline{q}^{\mathrm{c}}$, and $\overline{q}^{\mathrm{c}}$ are positive constants satisfying $\underline{q}^{\mathrm{s}} < \overline{q}^{\mathrm{s}}$ and $\underline{q}^{\mathrm{c}} < \overline{q}^{\mathrm{c}}$.

Let $E(v_p) \subseteq E$ denote the set of indices of the members that are connected to node $v_p \in V$. Condition (ii) requires that S should satisfy

$$|S \cap E(v_p)| \leq 1, \quad \forall v_p \in V. \tag{3}$$

Note that all members connected to a node of the initial structure can possibly be removed; such a node satisfies $|S \cap E(v_p)| = 0$. Constraint (3) allows the existence of a node connected only to cables. Such a node is forbidden by condition (ii), i.e., if no strut is connected to node v_p, then no cable is connected to v_p. This constraint is formally written as

$$S \cap E(v_p) = \emptyset \Rightarrow C \cap E(v_p) = \emptyset \quad (\forall v_p \in V). \tag{4}$$

It is easy to verify that condition (ii) is equivalent to (3) and (4).

We also consider the lower bound constraint on the number of struts as a parameter, which can be written as

$$|S| \geq \bar{s}, \tag{5}$$

where $\bar{s}$ is the specified value. In designing a tensegrity structure, we will use $\bar{s}$ as a parameter to generate various configurations. For instance, if $\bar{s} = \lfloor |V|/2 \rfloor$, then the generated tensegrity structure uses as many nodes as possible. Roughly speaking, the volume of space covered by a tensegrity structure increases as $\bar{s}$ increases.

Presence of mutually intersecting members in a tensegrity structure is not accepted, although an initial structure used in the ground structure method usually includes many intersecting candidate members. From a practical point of view, two members that are too close should not exist simultaneously. Let $\delta > 0$ denote the lower bound for the distance of existing members. We write $(i, i') \in P_{\mathrm{cross}}$ if the distance of member i and member i' is less than δ. The constraint excluding too close members is formally written as

$$\{i, i'\} \not\subseteq S \cup C, \quad \forall (i, i') \in P_{\mathrm{cross}}. \tag{6}$$

In this section, we have seen that conditions (i) and (ii) are formally stated as (2), (3), and (4). These constraints, as well as constraints (5) and (6), will be explicitly dealt with by introducing some integer variables; see section 2.2. In contrast, condition (iii) is not addressed as a constraint of the optimization problem to be solved. However, it will be shown through numerical experiments that we often obtain a solution satisfying condition (iii) by solving the optimization problem proposed in section 5.

2.2 Integer variables for labeling members

As explained in section 2.1, topology of a tensegrity structure is determined by finding a partition of E into disjoint subsets $E = S \cup C \cup N$ satisfying constraints (1)–(6). In other words, each member of the initial structure is to be classified into either S, C, or N. A key idea proposed in [18, 19] to express this classification in an optimization problem is making use of integer

variables that serve as labels of members. Specifically, we use two 0–1 variables, x_i and y_i, to express the label of member i as

$$(x_i, y_i) = (1, 0) \quad \Leftrightarrow \quad i \in S, \tag{7a}$$
$$(x_i, y_i) = (0, 1) \quad \Leftrightarrow \quad i \in C, \tag{7b}$$
$$(x_i, y_i) = (0, 0) \quad \Leftrightarrow \quad i \in N. \tag{7c}$$

By using (7), constraints (2), (3), (4), (5), and (6) can be rewritten as linear inequalities as follows. For each $i \in E$, constraint (2) is equivalent to

$$-\overline{q}^{\mathrm{s}} x_i \leq q_i \leq -\underline{q}^{\mathrm{s}} x_i + \overline{q}^{\mathrm{c}}(1 - x_i), \tag{8a}$$
$$\underline{q}^{\mathrm{c}} y_i - \overline{q}^{\mathrm{s}}(1 - y_i) \leq q_i \leq \overline{q}^{\mathrm{c}} y_i. \tag{8b}$$

The discontinuity constraint of struts, (3), is equivalent to

$$\sum_{i \in E(v_p)} x_i \leq 1, \quad \forall v_p \in V. \tag{9}$$

The constraint excluding nodes connected only to cables, (4), is equivalently rewritten as

$$y_i \leq \sum_{i' \in E(v_p)} x_{i'} \ (\forall i \in E(v_p)), \quad \forall v_p \in V, \tag{10}$$

Furthermore, constraint (5) is equivalent to

$$\sum_{i \in E} x_i \geq \bar{s}, \tag{11}$$

and constraint (6) is equivalent to

$$x_i + x_{i'} + y_i + y_{i'} \leq 1, \quad \forall (i, i') \in P_{\mathrm{cross}}. \tag{12}$$

See [18, 19] for details. It is worth noting that (8), (9), (10), (11), and (12) are tractable constraints, because they are linear constraints on $\boldsymbol{q}$, $\boldsymbol{x}$, and $\boldsymbol{y}$. Only the integrality constraints on $\boldsymbol{x}$ and $\boldsymbol{y}$ are intractable. Therefore, the constraints considered in this section can be treated within the framework of MILP.

3 Different member lengths: implicit constraint on symmetry

In general, symmetry of structures provides both practical and theoretical advantages in applications. It is also related to beauty and simplicity. In particular, many well-known tensegrity structures have symmetric configurations such that nodes are located at vertices of (semi-)regular polyhedron [4, 5, 15, 26]. On the other hand, for diversity of tensegrity structures found by a design approach, it is favorable that a design space is not limited to symmetric configurations. Indeed, design methods for finding non-symmetric tensegrity structures have gotten much attention recently [22, 30, 41, 44]. This section discusses constraints for generating solutions with/without various symmetries in the framework of topology optimization. Symmetry of optimal solutions in structural optimization has recently been of particular interest [11, 32, 35, 40].

Symmetry of a structure is an invariance property of its geometry with respect to a certain transformation, e.g., reflection across a plane or rotation around an axis. Since locations of the nodes are specified in a conventional ground structure method, symmetry of a solution is expressed as invariance of the vector of cross-sectional areas with respect to a certain permutation of its elements. Therefore, if we specify the symmetry property of a solution in advance, then the constraints on symmetry can be written as linear equality constraints on member cross-sectional areas. However, we do not adopt this explicit constraint of symmetry. For an arbitrary specified symmetry property, the design problem of tensegrity structures does not necessarily feasible. Hence, we cannot know, in advance, symmetry of tensegrity structures that can be obtained from a given initial structure. Moreover, when we attempt to find non-symmetric structures, symmetric structures are not excluded with this explicit constraint, because a solution with high symmetry is feasible for the constraint on lower symmetry. This yields disadvantage in diversity of configurations obtained by a design approach. For these reasons, we do not impose explicit restriction of specified symmetry. Rather, we introduce a constraint which can control symmetry of solutions in an implicit way.

An essential idea for controlling symmetry of a solution is to specify the number of different member lengths of the solution. For instance, consider the problem in Figure 1. Figure 1(a) depicts an initial truss endowed with the D_8-symmetry in the Schoenflies notation. The nodes are located at the vertices of two horizontal congruent regular octagons. The upper octagon is rotated counter-clockwise around the vertical axis at an angle of $\pi/6$. Any two nodes are connected by a member but only some of them are shown in Figure 1(a). Thus the geometry of this initial structure is symmetric with respect to the dihedral group of degree 8, i.e.,

$$\mathrm{D}_8 = \{r(2\pi i/8), \sigma r(2\pi i/8) \mid i = 0, 1, \ldots, 7\},$$

where $r(2\pi i/8)$ denotes a rotation about the X_3-axis at an angle of $2\pi i/8$ and σ is the half-rotation about the X_2-axis. Two tensegrity structures obtained from this initial structure are illustrated in Figure 1(b) and Figure 1(c), where the thick lines represent struts and the thin lines are cables. Both tensegrity structures consist of 8 struts and 32 cables. A key observation is that high symmetry implies a small number of different member lengths. In Figure 1(b), all struts have the same length and the configuration of the structure has D_8-symmetry. In contrast, in Figure 1(c), the tensegrity structure has four longer struts and four shorter struts, i.e., the number of different strut lengths is two. Accordingly, the configuration of this structure has lower symmetry than D_8; it has D_4-symmetry.

As demonstrated by the example, high symmetry in geometry implies that the number of different member lengths is small. As the contrapositive, if the number of different member lengths is large, then the geometry of the structure has low symmetry. For instance, if all members have different lengths, then it is clear that geometry of the structure has no symmetry. The inverse of this assertion is not necessarily true. Even if the number of different member lengths is small, the geometry of the structure can possibly have only low symmetry.[1] In other words, specifying a small number of different member lengths in structural optimization does not

[1] A tensegrity structure with a few number of different member lengths was called a *semiregular tensegrity structure* by Zhang *et al.* [44].

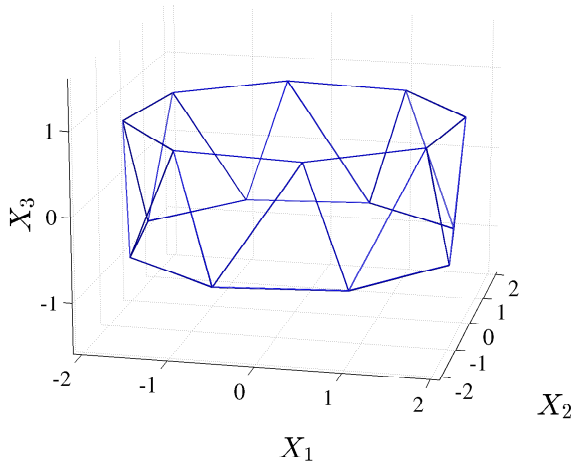

(a)

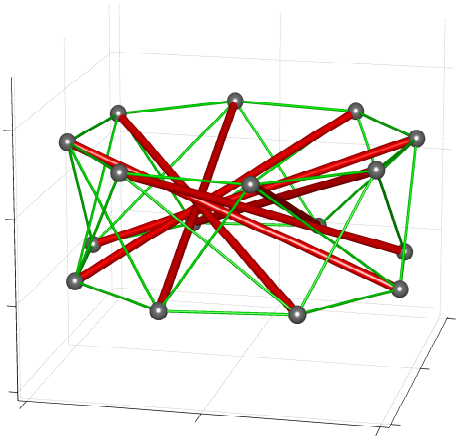

perspective

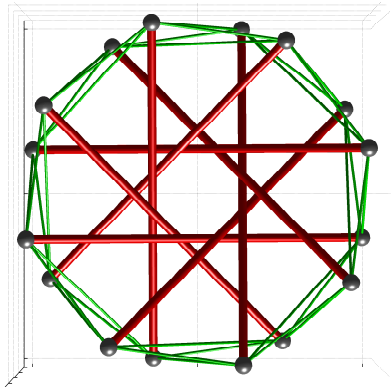

plan

(b)

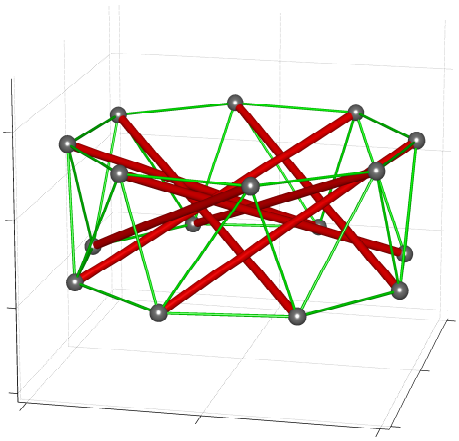

perspective

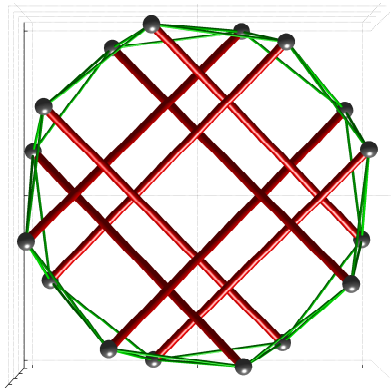

plan

(c)

Figure 1: Symmetry of structures and number of different member lengths. (a) Locations of nodes of the initial structure; (b) a D_8-symmetric solution with uniform strut lengths and three different cable lengths; and (c) a D_4-symmetric solution with two different strut lengths and three different cable lengths.

guarantee high symmetry of the optimal solution. Nonetheless, numerical examples in section 6 will demonstrate that symmetric solutions are often obtained by specifying a small number of different member lengths.

In the following, we consider only the number of different strut lengths, denoted by $\bar{b}$. The constraint on the number of different cable lengths can certainly be dealt with in the same manner.

Let l_i denote the length of member i of the initial structure. Since the coordinate of nodes of the initial structure are specified, l_i is constant. Let $E_j \subseteq E$ be a set of members that have the same member lengths. In other words, $i \in E_j$ and $i' \in E_j$ imply $l_i = l_{i'}$; conversely, if $l_i = l_{i'}$, then there exists j such that $i \in E_j$ and $i' \in E_j$. Suppose that the initial structure has b different member lengths. Then we obtain a partition of E into b disjoint subsets:

$$E = E_1 \cup \cdots \cup E_b. \tag{13}$$

We write $B = \{1, \ldots, b\}$ for simplicity. Formally, E_j $(j \in B)$ are defined as follows. Let $\sim$ be an equivalence relation on E defined as the symmetric and transitive closure of the binary relation:

$$i \sim i' \quad \Leftrightarrow \quad l_i = l_{i'},$$

where $i \sim i$ for all $i \in E$ by convention. Then the partition in (13) is obtained as the partition of E into equivalence classes induced by $\sim$. Define 0–1 variables z_j $(j \in B)$ by

$$z_j = \begin{cases} 0 & \text{if } S \cap E_j = \emptyset, \\ 1 & \text{if } S \cap E_j \neq \emptyset. \end{cases} \tag{14}$$

Then the constraint of the number of different strut lengths can be written as

$$\sum_{j \in B} z_j = \bar{b}, \tag{15}$$

where $\bar{b}$ is a specified value.

Constraint (14) can be treated within the framework of MILP by using the member labels, x_i $(i \in E)$. Recall (7) to see that $x_i = 1$ if $i \in S$, otherwise $x_i = 0$. Therefore, $\sum_{i \in E_j} x_i$ is equal to the number of struts belonging to E_j. From this observation it follows that (14) is equivalently rewritten as

$$z_j = \begin{cases} 0 & \text{if } \displaystyle\sum_{i \in E_j} x_i = 0, \\ 1 & \text{if } \displaystyle\sum_{i \in E_j} x_i \geq 1. \end{cases} \tag{16}$$

Finally, since $x_i \in \{0, 1\}$, (16) is equivalent to

$$z_j \leq \sum_{i \in E_j} x_i, \tag{17a}$$

$$z_j \geq \frac{1}{|E_j|} \sum_{i \in E_j} x_i, \tag{17b}$$

$$z_j \in \{0, 1\}, \tag{17c}$$

where $|E_j|$ is the number of members belonging to E_j.

The upshot of this section is that the constraint on the number of different strut lengths can be written as (15) and (17). The solution has low, or no, symmetry if $\bar{b}$ is large, while $\bar{b}$ is small if the solution has high symmetry.

4 Kinematical indeterminacy

Constraints for statical and kinematical indeterminacy of tensegrity structures are formulated based upon the Maxwell counting rule.

4.1 Maxwell's counting rule

Let d_{k} and d_{s} denote the degree of kinematical indeterminacy and the degree of statical indeterminacy, respectively. Since a tensegrity structure is a prestressed structure, it satisfies $d_{\mathrm{s}} \geq 1$. Moreover, this paper concerns kinematically indeterminate tensegrity structures, and hence $d_{\mathrm{k}} \geq 1$ should be satisfied. These constraints are dealt with based upon the Maxwell counting rule for rigidity [4, 6, 28], which is briefly recalled in this section.

The force-balance equation of the initial structure is written as (1), where the equilibrium matrix H is a $3|V| \times |E|$ matrix. Since the vector of self-equilibrium forces is a nontrivial solution of (1), the number of states of self-stress, d_{s}, is given by

$$d_{\mathrm{s}} = |E| - \operatorname{rank} H. \tag{18}$$

On the other hand, the compatibility relations can be written as

$$H^{\top} \boldsymbol{u} = \boldsymbol{e}, \tag{19}$$

where $\boldsymbol{u} \in \mathbb{R}^{3|V|}$ is the displacements vector and $\boldsymbol{e} \in \mathbb{R}^{|E|}$ is the vector of member elongations. An inextensional deformation is identified as a nontrivial solution of (19) with $\boldsymbol{e} = \boldsymbol{0}$. Hence, the number of infinitesimal mechanisms, d_{k}, is given by

$$d_{\mathrm{k}} = 3|V| - \operatorname{rank} H^{\top} - 6, \tag{20}$$

because the number of degrees of freedom of rigid body motion is six. Since $\operatorname{rank} H = \operatorname{rank} H^{\top}$, subtracting (18) from (20) yields

$$d_{\mathrm{k}} - d_{\mathrm{s}} = 3|V| - |E| - 6. \tag{21}$$

This equality is known as the Maxwell counting rule [4, 6]. It is worth of noting that the mechanisms detected by Maxwell's rule may be either infinitesimal or finite. Issues of distinction between infinitesimal and finite mechanisms are not taken into account in this paper.

Condition (21) is formulated for a given initial structure. In a topology optimization problem to be solved, however, the number of nodes and the number of members of a tensegrity structure are unknown. In section 4.2 we rewrite (21) for a tensegrity structure by using the design variables.

4.2 Constraint for kinematical indeterminacy

We reformulate the Maxwell counting rule for the initial structure, (21), for a tensegrity structure. Since the number of members of a tensegrity structure is the sum of the number of struts and the number of cables, $|E|$ in (21) is to be replaced by $|S| + |C|$. Since condition (ii) in section 2.1 is satisfied by definition, the number of nodes, $|V|$, can be written as $2|S|$. By substituting these conditions, (21) is reduced to

$$d_{\mathrm{k}} - d_{\mathrm{s}} = 5|S| - |C| - 6. \tag{22}$$

As explained in section 2.1, we specify the lower bound for the number of struts, (5), in the design problem. Since struts have nonzero axial forces as described in (2), $\boldsymbol{q} \neq \boldsymbol{0}$ holds for any feasible solution. This means that the force-balance equation, (1), has a nontrivial solution, and hence $d_{\mathrm{s}} \geq 1$. Therefore, if we add the constraint

$$d_{\mathrm{k}} - d_{\mathrm{s}} \geq 0,$$

then $d_{\mathrm{k}} \geq 1$ is guaranteed, i.e., kinematical indeterminacy is guaranteed.

With the observation above, we consider the equality constraint

$$5|S| - |C| - 6 = \bar{d}, \tag{23}$$

where $\bar{d} \geq 0$ is the specified value of $d_{\mathrm{k}} - d_{\mathrm{s}}$. By using the 0–1 variables, x_i and y_i, introduced in section 2.2, (23) can be written as

$$\sum_{i \in E} (5x_i - y_i) - 6 = \bar{d}. \tag{24}$$

4.3 Exploration procedure

To find tensegrity structures, we solve an optimization problem, a complete formulation of which will be presented in section 5. The constraints of this optimization problem have been discussed in section 2.2 through section 4.2. These constraints include the following three constants:

- $\bar{s}$ in (11): The lower bound for the number of struts.
- $\bar{b}$ in (15): The number of different strut lengths.
- $\bar{d}$ in (24): Difference between the degrees of kinematical indeterminacy and statical indeterminacy.

With these parameters we propose a procedure for finding various tensegrity structures from a given initial structure. The optimal solution has more members as $\bar{s}$ increases. In conjunction with the objective function introduced in section 5, $\bar{s}$ roughly measures the volume of space occupied by a tensegrity structure. Parameter $\bar{b}$ manages symmetry, i.e., the optimal solution has less symmetry as $\bar{b}$ increases. As discussed below, parameter $\bar{d}$ is used for seeking a structure with unique state of self-stress and (some) inextensional mechanisms. By varying these three parameters various tensegrity structures can be gerated from one initial structure, which will be actually demonstrated in section 6.

Tensegrity structures are explored as follows. We choose $\bar{s}$ and $\bar{b}$ according to demand of size and symmetry of the solution. As discussed in section 4.2, $\bar{d}$ should be nonnegative to guarantee kinematical indeterminacy. Suppose that we start with $\bar{d} = 0$. From the observation in section 4.2, the optimal solution, if any, has $d_{\rm s} \geq 1$. If $d_{\rm s} = 1$, then $\bar{d} = 0$ implies $d_{\rm k} = 1$. This means that a kinematically indeterminate tensegrity structures with unique state of self-stress is successfully obtained, and we may move to the other values of $\bar{s}$ and $\bar{b}$. If $d_{\rm s} \geq 2$, i.e., if the state of self-stress is not unique, then we increase $\bar{d}$ and solve the optimization problem again. As observed in (23), increase of $\bar{d}$ means decrease of the number of cables, provided that the number of struts is constant. Therefore, we might expect that $d_{\rm s}$ decreases as $\bar{d}$ increases. If the optimal solution with $\bar{d} = 1$ satisfies $d_{\rm s} = 1$, then we terminate with success. In this case this solution has $d_{\rm k} = 2$ inextensional mechanisms. If the optimal solution with $\bar{d} = 1$ has $d_{\rm s} \geq 2$, then we next examine $\bar{d} = 2$. This procedure is repeated until we find a solution satisfying $d_{\rm s} = 1$. Note that we begin with $\bar{d} = 1$ in the numerical experiments in section 6; if $\bar{d} = 1$ is infeasible, then we examine $\bar{d} = 0$.

It is worth of noting that the procedure presented above is heuristic in the sense that it does not necessarily find a kinematically indeterminate tensegrity structures with unique state of self-stress. For instance, suppose that the optimal solution with $\bar{d} = 1$ has $d_{\rm s} \geq 2$. Then we proceed to $\bar{d} = 2$, but it is possible that the optimization problems with $\bar{d} \geq 2$ are infeasible. In such a case the proposed procedure fails. However, it will be demonstrated that the proposed procedure terminates with success in all numerical examples of section 6.

The geometrical nonlinearity is not taken into account in this procedure. Therefore, it is possible that the obtained tensegrity structure is not stabilized by introducing prestress forces. Nonetheless, in most every case in section 6, the tangent stiffness matrix of the tensegrity structure with the obtained prestress forces is positive definite, i.e., the tensegrity structure is prestress stable.

5 Optimization problem and its MILP reformulation

We solve a topology optimization problem in the exploration procedure proposed in section 4.3. This optimization problem is formulated as an MILP problem in this section.

As for the objective function, we may consider several different candidates. In this paper we do not attempt to optimize, or improve, any structural performance, e.g., structural stiffness. It was demonstrated in [18, 19] that optimizing the stiffness, i.e., minimizing the compliance, usually results in a kinematically determinate tensegrity structure. Rather, we attempt to find kinematically indeterminate tensegrity structures, as already mentioned. Among some possibilities, we choose to minimize the total length of cables. Recall that we consider the lower bound for the number of struts, i.e., $\bar{s}$ in (5). Roughly speaking, the volume of space occupied by a tensegrity structure is approximately proportional to the sum of member lengths. By minimizing the total length of cables, the number of struts tend to decrease. Moreover, cables connecting far-distant nodes tends to be removed, and thence the size of a tensegrity structure also tends to decrease. Thus, with this objective function parameter $\bar{s}$ serves as a rough measure of the volume of space occupied by a tensegrity structure.

According to the definition of tensegrity structure, we consider constraints (1), (2), (3), (4), (5), and (6) introduced in section 2.1. Regarding symmetry, the constraint on the number of different strut lengths has been introduced in section 3. The constraint for kinematical indeterminacy has been formulated in section 4. In addition to these, we consider the constraints that each strut should be connected to at least three cables. This is because existence of a strut connecting to only one or two cables might cause difficulty in fabrication of a tensegrity structure and instability even in the presence of prestress. This constraint is written as

$$|C \cap E(v_p)| \geq 3 \quad \Leftarrow \quad |S \cap E(v_p)| \geq 1 \tag{25}$$

for each node $v_p \in V$.

By summing up all these constraints and the objective function, the optimization problem that we solve is formulated as

$$\min_{S,C,\boldsymbol{z},\boldsymbol{q}} \quad \sum_{i \in C} l_i \tag{26a}$$

$$\text{s.t.} \quad H\boldsymbol{q} = \boldsymbol{0}, \tag{26b}$$

$$q_i \in \begin{cases} [-\overline{q}^{\mathrm{s}}, -\underline{q}^{\mathrm{s}}] & \text{if } i \in S, \\ [\underline{q}^{\mathrm{s}}, \overline{q}^{\mathrm{c}}] & \text{if } i \in C, \\ \{0\} & \text{if } i \notin S \cup C, \end{cases} \tag{26c}$$

$$|S \cap E(v_p)| \leq 1, \qquad \forall v_p \in V, \tag{26d}$$

$$|S \cap E(v_p)| \geq 1 \Leftarrow |C \cap E(v_p)| \geq 1, \quad \forall v_p \in V, \tag{26e}$$

$$|S| \geq \bar{s}, \tag{26f}$$

$$\{i, i'\} \not\subseteq S \cup C, \qquad \forall (i, i') \in P_{\mathrm{cross}}, \tag{26g}$$

$$\sum_{j \in B} z_j = \bar{b}, \tag{26h}$$

$$z_j = \begin{cases} 0 & \text{if } S \cap E_j = \emptyset, \\ 1 & \text{otherwise}, \end{cases} \qquad \forall j \in B, \tag{26i}$$

$$5|S| - |C| - 6 = \bar{d}, \tag{26j}$$

$$|C \cap E(v_p)| \geq 3 \Leftarrow |S \cap E(v_p)| \geq 1, \quad \forall v_p \in V, \tag{26k}$$

where S and C are disjoint subsets of E. Thus the design problem of tensegrity structures is determining member labels, S, C, and $N = E \setminus S \cup C$, and prestress forces, $\boldsymbol{q}$. The labels are expressed by using the 0–1 variables, x_i and y_i ($i \in E$). Then constraints (26c), (26d), (26e), (26f), and (26g) are rewritten as linear inequality constraints (8), (9), (10), (11), and (12) in section 2.2. Constraint (26i) is rewritten with x_i and y_i as (17) in section 3. Constraint (26j) is reduced to (24) in section 4.2. Regarding constraint (26k), observe that $|S \cap E(v_p)| = \sum_{i \in E(v_p)} x_i$ and $|C \cap E(v_p)| = \sum_{i \in E(v_p)} y_i$. Moreover, (26d) implies $|S \cap E(v_p)| = \sum_{i \in E(v_p)} x_i \in \{0, 1\}$. Therefore, (26k) can be rewritten as

$$\sum_{i \in E(v_p)} y_i \geq 3 \sum_{i \in E(v_p)} x_i, \quad \forall v_p \in V.$$

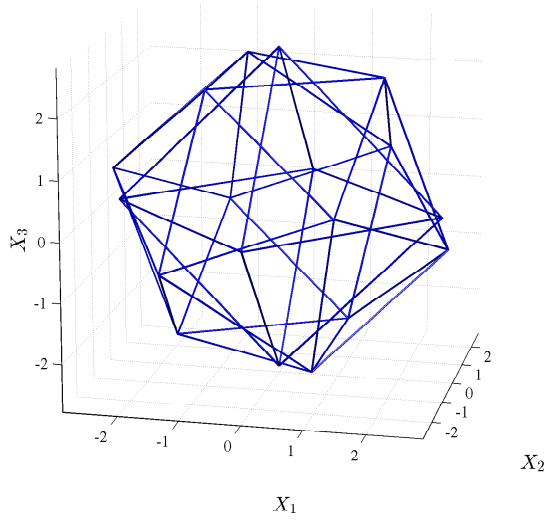

Figure 2: An 18-node initial structure of Example 1.

Table 1: Computational results of Example 1 with $\bar{b} = 2$ different strut lengths (Figure 3).

						CPU (s)	
$(\bar{s}, \bar{d}, \bar{b})$	$\lvert S\rvert$	$\lvert C\rvert$	d_{s}	d_{k}	$\sum_{i\in C} l_i$ (m)	CPLEX	Gurobi
$(7, 1, 2)$	7	28	1	2	82.263535	398.1	376.8
$(6, 1, 2)$	6	23	2	3	66.013237	223.4	281.6
$(6, 2, 2)$	6	22	1	3	65.981429	273.0	470.3
$(5, 1, 2)$	5	18	1	2	54.334314	209.3	566.0

Thus, all constraints of problem (26) can be rewritten as linear constraints in terms of 0–1 variables, $\boldsymbol{x}$, $\boldsymbol{y}$, and $\boldsymbol{z}$, and continuous variables, $\boldsymbol{q}$. The objective function in (26a) is rewritten as $\sum_{i\in E} l_i y_i$, which is also a linear function. Accordingly, problem (26) can be reduced to an MILP problem.

The full description of this MILP problem appears in appendix A.

6 Numerical experiments

The various tensegrity structures are found by solving MILP problem (27). Computation was carried out on two 2.66 GHz 6-Core Intel Xeon Westmere processors with 64 GB RAM. The data of MILP problem (27) were prepared with MATLAB Ver. 7.13 in the CPLEX LP file format. Then the MILP problem was solved by using CPLEX Ver. 12.2 [16] and Gurobi Optimizer Ver. 4.6 [12] for comparison. The tolerance of integrality feasibility of each solver was set as 10^{-8}. The other parameters are set as the default values. The bounds for prestress forces in (2) are $\underline{q}^{\mathrm{s}} = 5\,\mathrm{kN}$, $\overline{q}^{\mathrm{s}} = 100\,\mathrm{kN}$, $\underline{q}^{\mathrm{c}} = 5\,\mathrm{kN}$, and $\overline{q}^{\mathrm{c}} = 100\,\mathrm{kN}$.

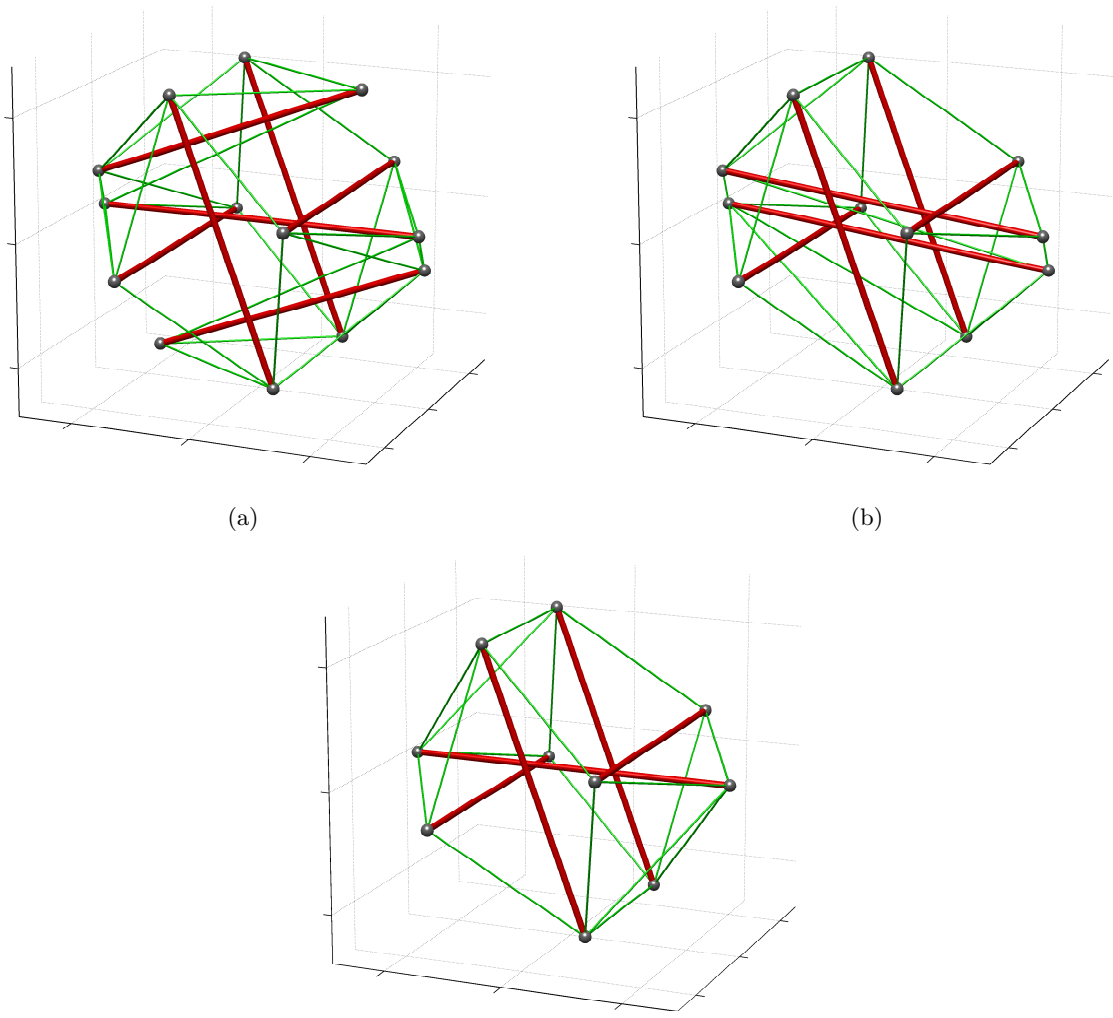

(a) (b)

(c)

Figure 3: Optimal solutions of Example 1 with $\bar{b} = 2$ different strut lengths. (a) $(\bar{s}, \bar{d}, \bar{b}) = (7, 1, 2)$; (b) $(\bar{s}, \bar{d}, \bar{b}) = (6, 2, 2)$; and (c) $(\bar{s}, \bar{d}, \bar{b}) = (5, 1, 2)$.

Table 2: Computational results of Example 1 with $\bar{b} = 3$ different strut lengths (Figure 4).

						CPU (s)	
$(\bar{s}, \bar{d}, \bar{b})$	$\lvert S\rvert$	$\lvert C\rvert$	d_{s}	d_{k}	$\sum_{i \in C} l_i$ (m)	CPLEX	Gurobi
$(9, 1, 3)$	9	38	1	2	97.893117	49,350.2	3,369.3
$(8, 1, 3)$	8	33	1	2	87.665780	6,715.7	2,694.6
$(7, 1, 3)$	7	28	1	2	76.446590	1,084.0	1,527.6
$(6, 1, 3)$	6	23	1	2	63.215175	1,627.8	1,248.2
$(5, 1, 3)$	5	18	1	2	52.015102	1,693.5	570.6

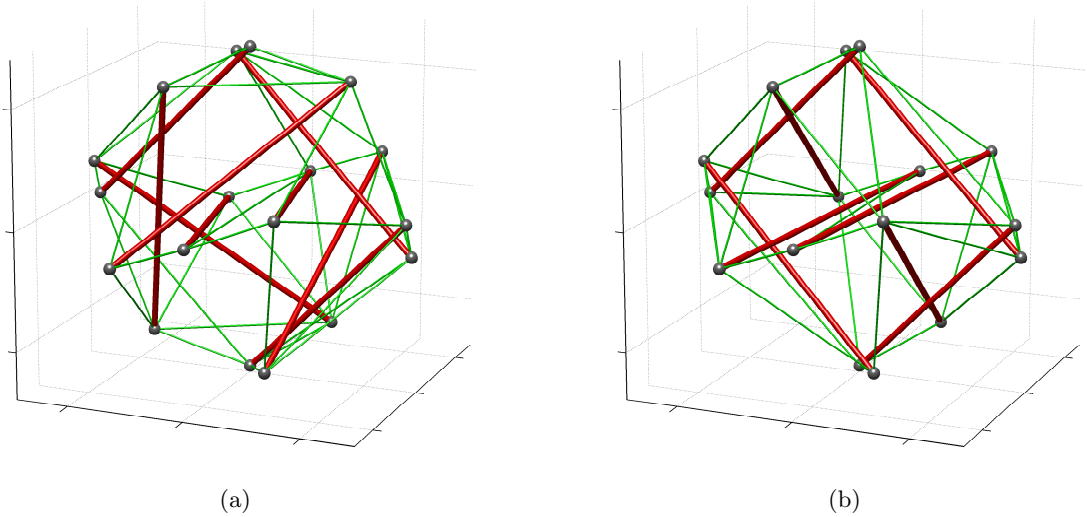

(a)

(b)

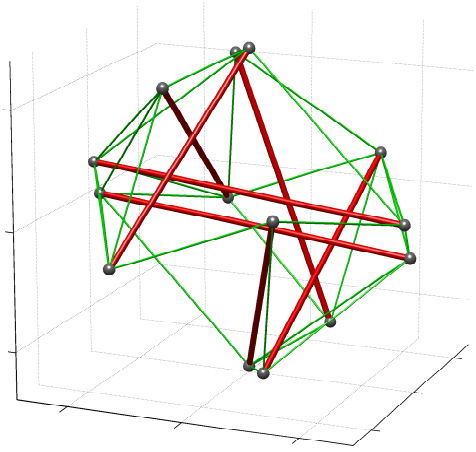

(c)

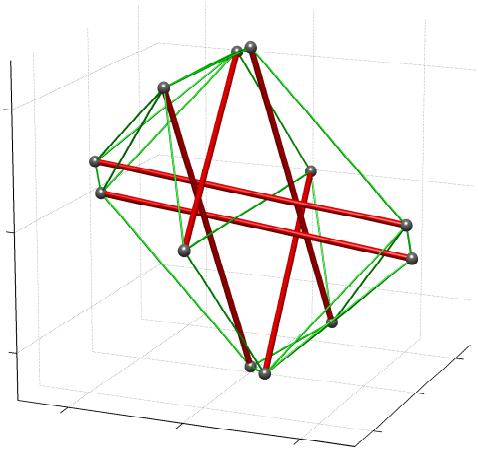

(d)

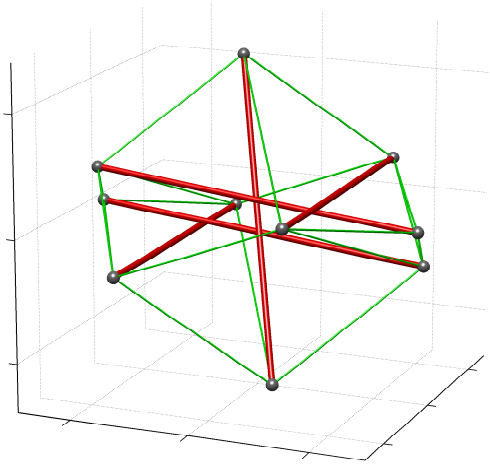

(e)

Figure 4: Optimal solutions of Example 1 with $\bar{b} = 3$ different strut lengths. (a) $(\bar{s}, \bar{d}, \bar{b}) = (9, 1, 3)$; (b) $(\bar{s}, \bar{d}, \bar{b}) = (8, 1, 3)$; (c) $(\bar{s}, \bar{d}, \bar{b}) = (7, 1, 3)$; (d) $(\bar{s}, \bar{d}, \bar{b}) = (6, 1, 3)$; and (e) $(\bar{s}, \bar{d}, \bar{b}) = (5, 1, 3)$.

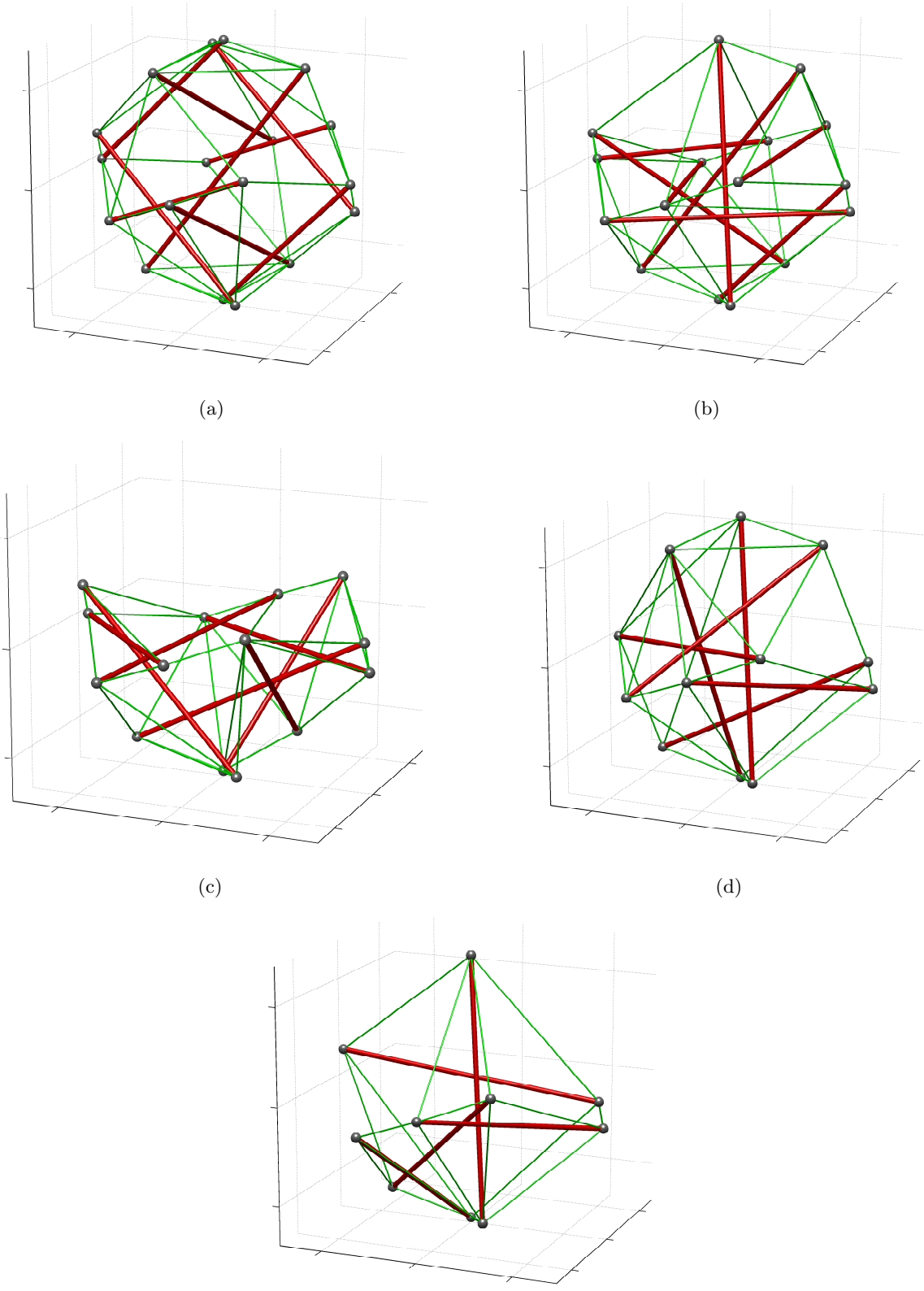

Figure 5: Optimal solutions of Example 1 with $\bar{b} = 5$ different strut lengths. (a) $(\bar{s}, \bar{d}, \bar{b}) = (9, 2, 5)$; (b) $(\bar{s}, \bar{d}, \bar{b}) = (8, 1, 5)$; (c) $(\bar{s}, \bar{d}, \bar{b}) = (7, 1, 5)$; (d) $(\bar{s}, \bar{d}, \bar{b}) = (6, 1, 5)$; and (e) $(\bar{s}, \bar{d}, \bar{b}) = (5, 1, 5)$.

Table 3: Computational results of Example 1 with $\bar{b} = 5$ different strut lengths (Figure 5).

						CPU (s)	
$(\bar{s}, \bar{d}, \bar{b})$	$\lvert S\rvert$	$\lvert C\rvert$	$d_{\rm s}$	$d_{\rm k}$	$\sum_{i\in C} l_i$ (m)	CPLEX	Gurobi
$(9, 1, 5)$	9	38	2	3	93.960131	613.8	1,147.4
$(9, 2, 5)$	9	37	1	3	91.252627	1,063.0	4,065.7
$(8, 1, 5)$	8	33	1	2	83.998252	17,157.7	13,810.8
$(7, 1, 5)$	7	28	1	2	73.852943	12,885.1	17,092.9
$(6, 1, 5)$	6	23	1	2	61.061823	6,240.1	10,987.7
$(5, 1, 5)$	5	18	1	2	50.690176	3,167.6	7,861.7

6.1 Example 1: 18-node initial structure

Consider an initial structure shown in Figure 2, where X_1 and X_2 are taken to be two horizontal axes and X_3 is the vertical axis. The structure consists of $|V| = 18$ nodes and $|E| = 153$ members.

The locations of the nodes of this initial structure are defined as the vertices of regular polyhedra centered at the origin. The 12 nodes are at vertices of a regular icosahedron with edge length 3 m, while the remaining 6 nodes are at vertices a regular octahedron with edge length $2.7\sqrt{2}$ m. Any two nodes are connected by a member, though only edges of polyhedra are illustrated in Figure 2. The number of different member lengths of this initial structure is $|B| = 22$. We define $P_{\rm cross}$ in (6) with the lower bound $\delta = 0.1$ m for the distance of two existing members. Then the initial structure includes $|P_{\rm cross}| = 292$ pairs of intersecting members. As a result, MILP problem (27) has $2|E|+|B| = 328$ binary variables, $|E| = 153$ continuous variables, 1444 linear inequality constraints, and 56 linear equality constraints.

As for the number of different strut lengths, $\bar{d}$, we consider three cases: $\bar{d} = 2$, 3, and 5. The optimal solutions for $\bar{d} = 2$ are shown in Figure 3, where the thick lines and the thin lines represent struts and cables, respectively. The computational results are listed in Figure 1, where $|S|$ is the number of struts, $|C|$ is the number of cables, $d_{\rm s}$ is the degree of statical indeterminacy, $d_{\rm k}$ is the degree of kinematical indeterminacy, $\sum_{i\in C} l_i$ is the optimal value (i.e., the total length of cables), and CPU is the computational time spent by an MILP solver. In each case, the number of struts becomes equal to its lower bound, $\bar{s}$. The same solutions are obtained by CPLEX and Gurobi Optimizer.

For $(\bar{s}, \bar{d}, \bar{b}) = (5, 1, 2)$ and $(7, 1, 2)$, the optimal solutions have only one state of self-stress, i.e., $d_{\rm s} = 1$. In contrast, the solution for $(\bar{s}, \bar{d}, \bar{b}) = (6, 1, 2)$ has $d_{\rm s} = 2$ states of self-stress. Hence, we examine the case of $(\bar{s}, \bar{d}, \bar{b}) = (6, 2, 2)$. Then the optimal solution, shown in Figure 3(b), satisfies $d_{\rm s} = 1$. The degree of kinematic indeterminacy is $d_{\rm k} = 3$. The configuration of this tensegrity structure is symmetric. Particularly, it has three pairs of parallel struts. The configurations of the tensegrity structures shown in Figure 3(a) and Figure 3(c) also have high symmetry. In this way, by choosing small $\bar{b}$, we can often obtain symmetric tensegrity structures. All tensegrity structures in Figure 3 are kinematically indeterminate (i.e., unstable). However, these tensegrity structures are stabilized by introducing the prestress forces (i.e., prestress stable). In other

words, the tangent stiffness matrices in the presence of prestress are positive definite.

If we set $(\bar{s}, \bar{b}) = (9, 2)$, then problem (27) has no feasible solution for any $\bar{d}$. For the $(\bar{s}, \bar{d}, \bar{b}) = (8, 1, 2)$, the optimal solution has $d_{\mathrm{s}} = 2$ states of self-stress. The optimal solution for $(\bar{s}, \bar{d}, \bar{b}) = (8, 2, 2)$ in turn has $d_{\mathrm{s}} = 1$. However, this solution is unstable even after introducing the prestress forces. Thus the optimal solution of problem (27) is not necessarily prestress stable. This is, on one hand, natural because we do not consider the constraint that the tensegrity structure is stabilized by prestress forces. However, on the other hand, it is very often that the optimal solution is prestress stable, as we shall see through the other examples in sections 6.1–6.3.

We next investigate cases with $\bar{d} = 3$ different strut lengths. The optimal solutions are collected in Figure 4 and the computational results are listed in Table 2. In most every case the computational time required by Gurobi Optimizer is less than that required by CPLEX. In particular, for the case $(\bar{s}, \bar{d}, \bar{b}) = (9, 1, 3)$ the computational time of CPLEX is more than 14 times larger. However, for $(\bar{s}, \bar{d}, \bar{b}) = (7, 1, 3)$, Gurobi Optimizer requires more computational time than CPLEX. All the solutions in Figure 4 have $d_{\mathrm{s}} = 1$ state of self-stress and $d_{\mathrm{k}} = 2$ inextensional mechanisms. They are prestress stable, i.e., they are stabilized by introducing the prestress forces. Configurations of the solutions for $\bar{s} = 8$, 6, and 5 have symmetry properties. However, in the cases of $\bar{s} = 9$ and 7, the obtained solutions are not symmetric. This illustrates that an asymmetric tensegrity structure can be kinematically indeterminate and prestress stable, although many of tensegrity structures in literature have some symmetry properties.

Figure 5 collects the optimal solutions with $\bar{b} = 5$ different strut lengths. All these tensegrity structures are prestress stable. The computational results are listed in Table 3. In most every case the computational time of CPLEX is less than that of Gurobi Optimizer. The only exception is the case of $(\bar{s}, \bar{d}, \bar{b}) = (8, 1, 5)$. For $(\bar{s}, \bar{d}, \bar{b}) = (8, 1, 5)$ and $(7, 1, 5)$, both solvers require about four hours. The solution for $(\bar{s}, \bar{d}) = (9, 1, 5)$ has $d_{\mathrm{s}} = 2$ states of self-stress. In turn, the solution for $(\bar{s}, \bar{d}, \bar{b}) = (9, 2, 5)$ successfully has only $d_{\mathrm{s}} = 1$ state of self-stress. In the configuration of this solution shown in Figure 5(a), alignment of the struts has a rotational symmetry property. However, the cables are not symmetric. All the other configurations in Figure 5 have no symmetry property. Thus, we obtain asymmetric tensegrity structures by increasing $\bar{b}$.

Study of the examples in this section demonstrates that, by changing parameters $\bar{s}$ and $\bar{b}$, we can obtain diverse configurations of tensegrity structures from one ground structure. We can often obtain a tensegrity structure with only one degree of statical indeterminacy by adjusting parameter $\bar{d}$.

6.2 Example 2: 22-node initial structure

We next consider an initial structure illustrated in Figure 6. This structure consists of $|V| = 22$ nodes and $|E| = 191$ members. The number of different member lengths is $|B| = 37$. The number of pairs of intersecting members is $|P_{\mathrm{cross}}| = 250$ when the threshold is $\delta = 0.1\,\mathrm{m}$.

Locations of the nodes of this initial structure are defined as the vertices of four horizontal polygons shown in Figure 6. The bottom and top polygons are equilateral triangles, while the middle two ones are regular octagons. The centers of these polygons are on the X_3-axis. The distance between a triangle and an octagon is 1 m, while the distance between two octagons is

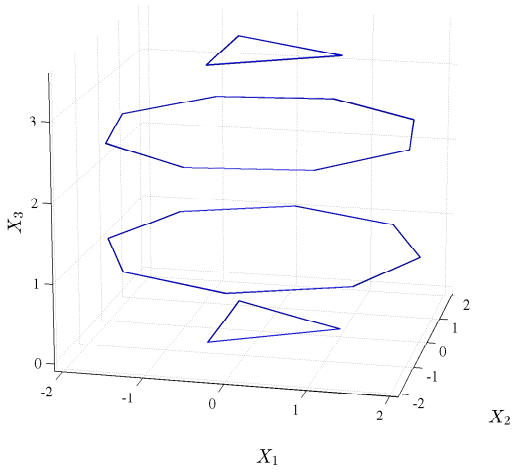

Figure 6: A 22-node initial structure of Example 2.

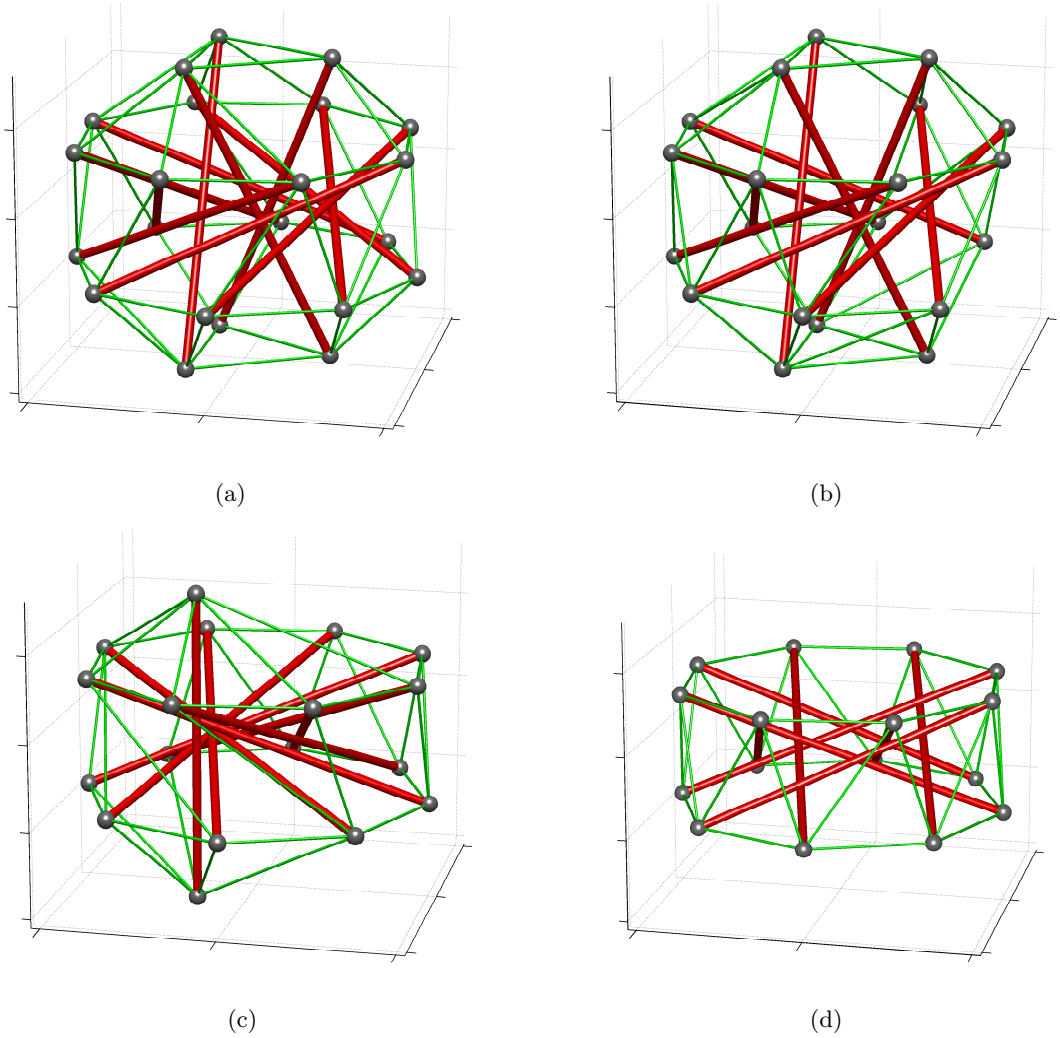

Figure 7: Optimal solutions of Example 2 with $\bar{b} = 2$ different strut lengths. (a) $(\bar{s}, \bar{d}, \bar{b}) = (11, 1, 2)$; (b) $(\bar{s}, \bar{d}, \bar{b}) = (10, 1, 2)$; (c) $(\bar{s}, \bar{d}, \bar{b}) = (9, 1, 2)$; and (d) $(\bar{s}, \bar{d}, \bar{b}) = (8, 2, 2)$.

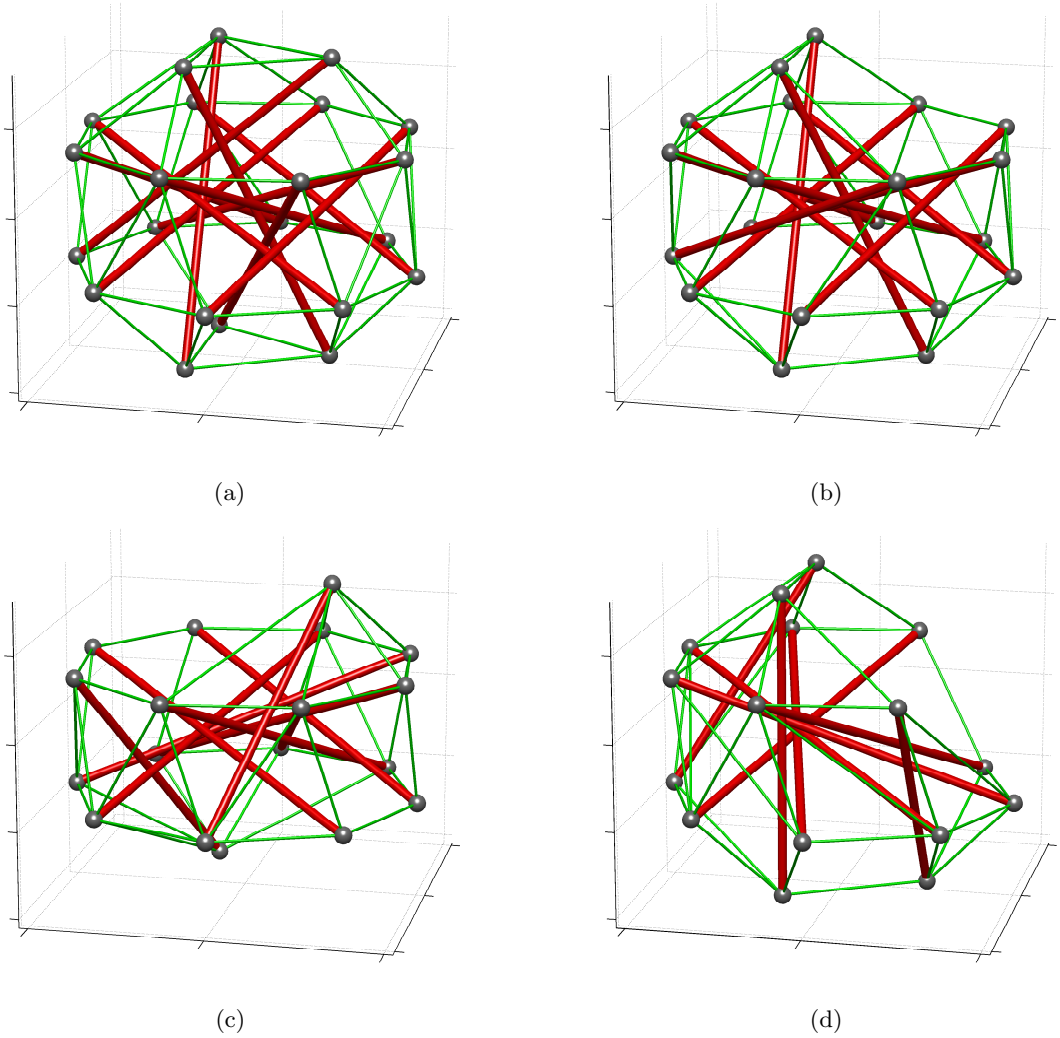

(a) (b) (c) (d)

Figure 8: Optimal solutions of Example 2 with $\bar{b} = 3$ different strut lengths. (a) $(\bar{s}, \bar{d}, \bar{b}) = (11, 1, 3)$; (b) $(\bar{s}, \bar{d}, \bar{b}) = (10, 2, 3)$; (c) $(\bar{s}, \bar{d}, \bar{b}) = (9, 1, 3)$; and (d) $(\bar{s}, \bar{d}, \bar{b}) = (8, 1, 3)$.

Table 4: Computational results of Example 2 with $\bar{b} = 2$ different strut lengths (Figure 7).

						CPU (s)	
$(\bar{s}, \bar{d}, \bar{b})$	$\lvert S\rvert$	$\lvert C\rvert$	d_{s}	d_{k}	$\sum_{i \in C} l_i$ (m)	CPLEX	Gurobi
$(11, 1, 2)$	11	48	1	2	78.809440	43.9	53.9
$(10, 1, 2)$	10	43	1	2	73.740650	4,991.4	588.7
$(9, 1, 2)$	9	38	1	2	66.858350	726.4	1,001.0
$(8, 1, 2)$	8	33	2	3	54.278517	17.1	175.0
$(8, 2, 2)$	8	32	1	3	51.778517	56.4	169.6

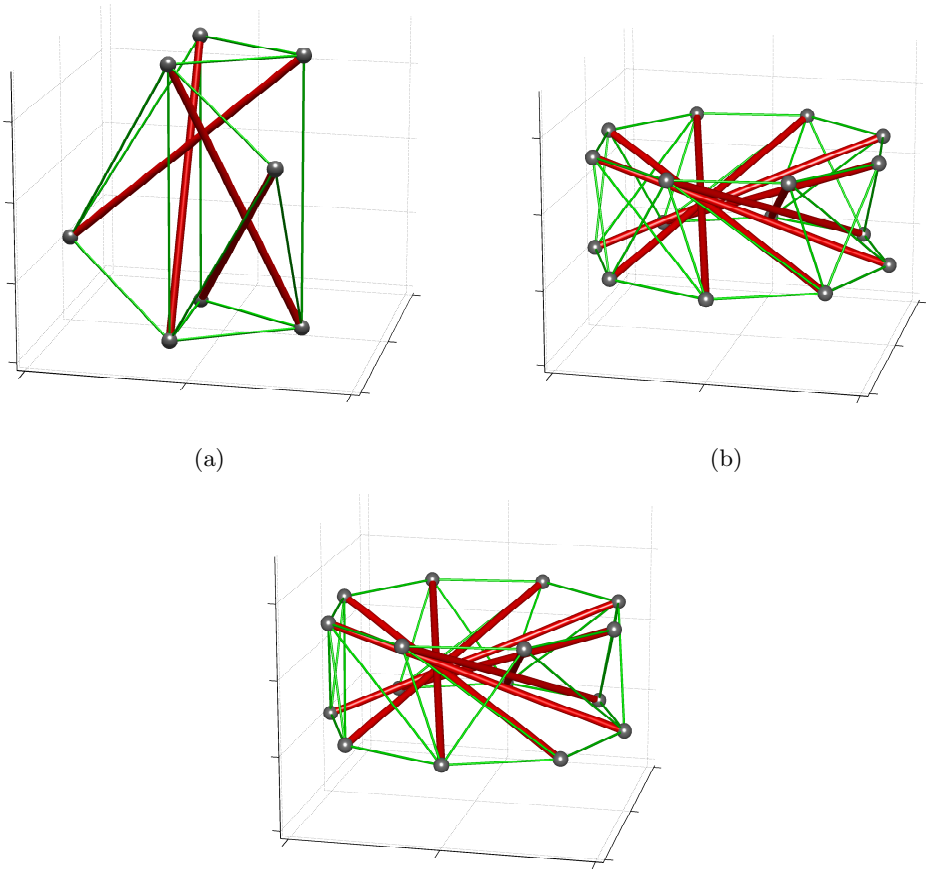

(a) (b)

(c)

Figure 9: Optimal solutions of Example 2 with uniform strut lengths ($\bar{b} = 1$). (a) $(\bar{s}, \bar{d}, \bar{b}) = (4, 0, 1)$; (b) $(\bar{s}, \bar{d}, \bar{b}) = (5, 1, 1)$; and (c) $(\bar{s}, \bar{d}, \bar{b}) = (8, 1, 1)$.

Table 5: Computational results of Example 2 with $\bar{b} = 3$ different strut lengths (Figure 8).

						CPU (s)	
$(\bar{s}, \bar{d}, \bar{b})$	$\lvert S\rvert$	$\lvert C\rvert$	d_{s}	d_{k}	$\sum_{i \in C} l_i$ (m)	CPLEX	Gurobi
$(11, 1, 3)$	11	48	1	2	77.517351	48.8	234.5
$(10, 1, 3)$	10	43	2	3	70.981031	1,082.0	1,365.0
$(10, 2, 3)$	10	42	1	3	68.481031	1,139.7	2,147.6
$(9, 1, 3)$	9	38	1	2	64.357465	2,960.0	4,713.3
$(8, 1, 3)$	8	33	1	2	58.268308	6,451.8	37,294.2

Table 6: Computational results of Example 2 with uniform strut lengths ($\bar{b} = 1$, Figure 9).

						CPU (s)	
$(\bar{s}, \bar{d}, \bar{b})$	$\lvert S\rvert$	$\lvert C\rvert$	$d_{\rm s}$	$d_{\rm k}$	$\sum_{i\in C} l_i$ (m)	CPLEX	Gurobi
$(4, 0, 1)$	4	14	1	1	35.325779	1.1	7.5
$(5, 1, 1)$	8	33	1	2	58.811663	7.0	7.8
$(8, 1, 1)$	8	33	1	2	58.811663	1.2	2.4

1.5 m. The length of an edge of a triangle is $\sqrt{3}$ m. An octagon is inscribed a circle with radius 2 m and the length of its edge is $2\sqrt{2-\sqrt{2}}$ m. Each triangle has an edge that is parallel to the X_2-axis. The lower octagon has two vertices on the X_1-axis, and the upper octagon is rotated counter-clockwise around the X_3-axis at an angle $\pi/6$. Any two nodes of the initial structure are connected by a member but diagonals of octagons are removed.

As for the number of different strut lengths, $\bar{d}$, we consider three cases: $\bar{d} = 1$, 2, and 3. The optimal solutions are shown in Figure 7, Figure 8, and Figure 9. The computational results are listed in Table 4, Table 5, and Table 6. It is observed that the computational time of CPLEX is less than that of Gurobi Optimizer in most every case. The only exception is the case of $(\bar{s}, \bar{d}, \bar{b}) = (10, 1, 2)$, where the computational time required by CPLEX is about eight times larger than that required by Gurobi Optimizer. In contrast, in the case of $(\bar{s}, \bar{d}, \bar{b}) = (8, 1, 3)$, the computational time of Gurobi Optimizer is about five times larger than that of CPLEX.

The optimal solutions for $\bar{b} = 2$ appear in Figure 7. It is observed that tensegrity structures with various configurations can be generated by changing $\bar{s}$. In the solution for $(\bar{s}, \bar{d}, \bar{b}) = (11, 1, 2)$ shown in Figure 7(a), alignment of struts has a symmetric property. More specifically, the set of longer three struts is symmetric with respect to the dihedral group D_3, i.e., it is symmetric with respect to the rotation around the X_3-axis at an angle of $2n\pi/3$ ($n = 0, 1, 2$) and the half-rotation about the X_1-axis. The set of eight remaining struts is symmetric with respect to D_8. The alignment of cables, however, has no symmetry property. In the solution for $(\bar{s}, \bar{d}, \bar{b}) = (10, 1, 2)$ shown in Figure 7(b), alignment of longer struts has D_3-symmetry, while alignment of the remaining seven shorter struts has no symmetry property. In contrast, the solution for $(\bar{s}, \bar{d}, \bar{b}) = (9, 1, 2)$ in Figure 7(c) has one longer strut and D_8-symmetric shorter struts. The solution for $(\bar{s}, \bar{d}, \bar{b}) = (8, 1, 2)$ has $d_{\rm s} = 2$ states of self-stress. Hence, we examine $\bar{d} = 2$. Then the obtained solution successfully has only one mode. This solution, shown in Figure 7(d), has four longer struts and four shorter struts. Alignment of cables has the same symmetry property as that of struts. Therefore, the configuration of this tensegrity structure is symmetric with respect to D_4.

Figure 8 collects the optimal solutions obtained for $\bar{b} = 3$. The solution for $(\bar{s}, \bar{d}, \bar{b}) = (10, 2, 3)$ has $d_{\rm k} = 3$ inextensional mechanisms, while the other solutions in Figure 8 have $d_{\rm k} = 2$ inextensional mechanisms. The optimal solutions for $\bar{b} = 1$ are collected in Figure 9. Note that problem (27) is infeasible for $\bar{s} \geq 9$ and $\bar{b} = 1$. The optimal solution for $(\bar{s}, \bar{d}, \bar{b}) = (4, 0, 1)$ in Figure 9(a) has no symmetry property. Since this solution has only $d_{\rm s} = 1$ state of self-stress, the case of $(\bar{s}, \bar{d}, \bar{b}) = (4, 1, 1)$ is not explored. For $(\bar{s}, \bar{d}, \bar{b}) = (5, 1, 1)$, the optimal solution has

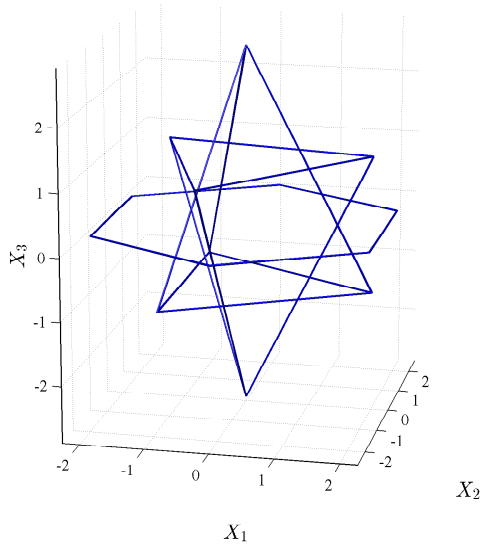

Figure 10: A 14-node initial structure of Example 3.

Table 7: Computational results of Example 3.

						CPU (s)	
$(\bar{s}, \bar{d}, \bar{b})$	$\lvert S\rvert$	$\lvert C\rvert$	d_{s}	d_{k}	$\sum_{i\in C} l_i$ (m)	CPLEX	Gurobi
$(7, 1, 3)$	7	28	1	2	72.048914	125,786.5	9,002.7
$(7, 1, 7)$	7	28	1	2	75.701727	40,356.6	4,225.0
$(6, 1, 2)$	6	23	3	4	64.255004	0.6	0.7
$(6, 2, 2)$	6	22	2	4	59.924877	0.6	0.8
$(6, 3, 2)$	6	21	1	4	55.594750	0.6	0.8
$(6, 1, 3)$	6	23	1	2	63.730829	5,730.8	591.6
$(6, 1, 6)$	6	23	1	2	60.948546	19,723.5	539.8

eight struts as shown in Figure 9(b). Alignment of struts of this solution is same as that of the solution for $(\bar{s}, \bar{d}, \bar{b}) = (8, 1, 1)$ and is D_8-symmetric. Finally, it is worth noting that all the solutions shown in Figure 7, Figure 8, and Figure 9 are prestress stable.

6.3 Example 3: 14-node initial structure

In this section we consider an initial structure shown in Figure 10. The structure consists of $|V| = 14$ nodes and $|E| = 91$ members.

Locations of the nodes of this initial structure are defined so that eight nodes form two regular tetrahedra with edge length $2\sqrt{3}\,\mathrm{m}$ and the remaining six nodes form a regular hexagon with edge length 2.5 m. The centers of the tetrahedra and hexagon are on the X_3-axis. The hexagon is parallel to the X_1X_2-plane. Each tetrahedron has a face that is parallel to the X_1X_2-plane. The distance between this bottom face of a tetrahedron and the octagon is 1 m. The bottom face of the inverted tetrahedron is rotated counter-clockwise around the X_3-axis at an angle of $\pi/9$ from the bottom face of the other tetrahedron. Any two nodes are connected by

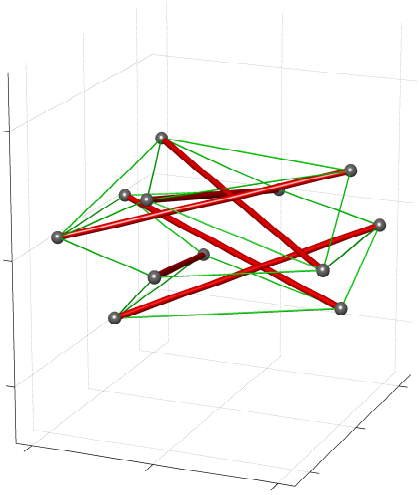

(a)

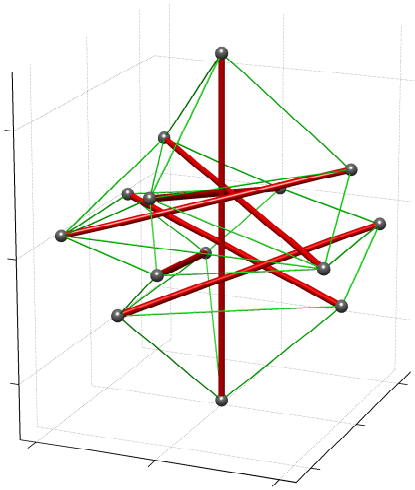

(b)

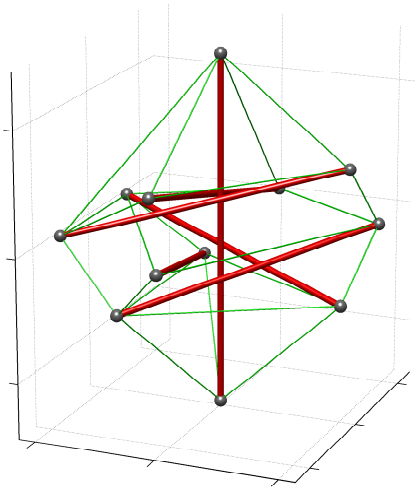

(c)

Figure 11: Optimal solutions of Example 3 with few different strut lengths. (a) $(\bar{s}, \bar{d}, \bar{b}) = (6, 3, 2)$; (b) $(\bar{s}, \bar{d}, \bar{b}) = (7, 1, 3)$; and (c) $(\bar{s}, \bar{d}, \bar{b}) = (6, 1, 3)$.

a member. The number of pairs of intersecting members is $|P_{\text{cross}}| = 63$. As a result, MILP problem (27) has $2|E| + |B| = 202$ binary variables, $|E| = 91$ continuous variables, 769 linear inequality constraints, and 44 linear equality constraints.

The optimal solutions with $\bar{d} = 2$ and $\bar{d} = 3$ appear in Figure 11. The computational results are listed in Table 7. The computational time in the cases of $(\bar{s}, \bar{b}) = (6, 2)$ is small, while that in the other cases is very large. The solution for $(\bar{s}, \bar{d}, \bar{b}) = (6, 1, 2)$ has $d_{\text{s}} = 3$ states of self-stress. The solution for $(\bar{s}, \bar{d}, \bar{b}) = (6, 2, 2)$ has $d_{\text{s}} = 2$, i.e., the solution still has an extra mode of self-stress. Therefore, we proceed to $(\bar{s}, \bar{d}, \bar{b}) = (6, 3, 2)$. The solution in this case, shown in Figure 11(a), successfully has unique mode of self-equilibrium force. The configuration of this solution is D_3-symmetric. In contrast, the solutions for $(\bar{s}, \bar{d}, \bar{b}) = (7, 1, 3)$ and $(\bar{s}, \bar{d}, \bar{b}) = (6, 1, 3)$ have no symmetry property as shown in Figure 11(b) and Figure 11(c). If the number of different strut lengths is equal to the number of struts, i.e., if $\bar{b} = |S|$, then it is guaranteed

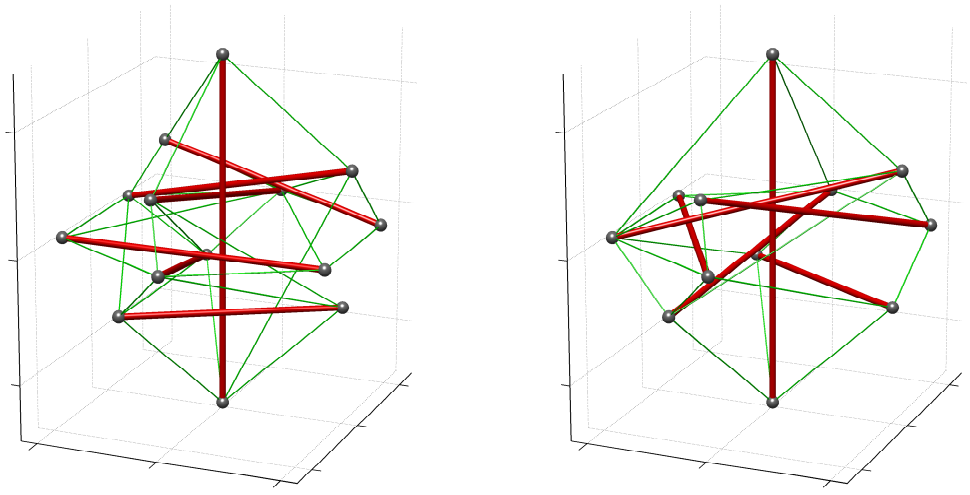

(a) (b)

Figure 12: Optimal solutions of Example 3 without same strut lengths. (a) $(\bar{s}, \bar{d}, \bar{b}) = (7, 1, 7)$ and (b) $(\bar{s}, \bar{d}, \bar{b}) = (6, 1, 6)$.

that the configuration of a tensegrity structure has no symmetry properties. Such examples are collected in Figure 12. All the tensegrity structures obtained in this section are prestress stable.

7 Summary and discussion

For developing innovative tensegrity structures in real applications, systematic approaches that can explore diverse topologies are desired. This paper have presented a numerical method for generating various topologies of tensegrity structures that satisfy the classical definition rigorously. The method is based upon truss topology optimization and does not require topology of tensegrity structures to be specified in advance. The optimization problem has been reduced to an MILP problem. Three parameters are used to generate many different topologies from one given initial structure. Difference between the degrees of kinematical indeterminacy and statical indeterminacy, $\bar{d}$, is used to guarantee kinematical indeterminacy and uniqueness of state of self-stress. The number of different strut lengths, $\bar{b}$, implicitly controls symmetry of a solution. In conjunction with the objective function that minimizes the total length of cables, the lower bound for the number of struts, $\bar{s}$, serves as a measure of the size of a solution. Numerical experiments have demonstrated that various tensegrity structures can be generated by varying these three parameters and that most of the obtained tensegrity structures are stabilized by introducing self-stress.

Some of the techniques developed in this paper are not restricted to tensegrity structures but applicable to generic truss topology optimization. For instance, the symmetry constraint by specifying the number of different member lengths may possibly be used in optimization of trusses with discrete cross-sectional areas. The optimal solution of such a nonconvex optimization problem is not necessarily symmetric, even if input data of the problem is symmetric [11, 32, 35, 40]. Under this situation the constraint on the number of different member lengths may possibly

impose symmetry of a solution to some extent. It is also relevant to standardization of components of a structure, and hence could be related to fabrication cost in real world problems. Note that, regarding symmetry only, we can consider the explicit constraint that members located in symmetric positions should have the same cross-sectional area. This explicit constraint and the implicit constraint considered in this paper might play complementary roles. The former can guarantee high symmetry but is not necessarily effective when solutions with low symmetry are desired. In contrast, the latter can guarantee low or no symmetry, but the small number of different member lengths does not necessarily imply high symmetry of a solution. These aspects remain to be further investigated.

Regarding design of tensegrity structures, much remains to be studied. For instance, it is not clear why minimizing the total length of cables, performed in this paper, often generates solutions that can be stabilized by self-stresses. Also, a remaining question is when a structure is simultaneously statically and kinematically indeterminate. Recently, conditions for determinacy and indeterminacy have been extensively studied for structures with symmetric configurations [6, 7, 9, 31, 33, 42]. However, the numerical examples presented in this paper illustrate that structures with non-symmetric configurations can be simultaneously statically and kinematically indeterminate. Sufficient conditions for simultaneous static and kinematical indeterminacy, as well as for prestress stability, of structures with non-symmetric configurations might be explored. Furthermore, the proposed method is based on MILP, which might be a potential disadvantage in computational cost for finding tensegrity structures consisting of a large number of members.

Acknowledgments

This work is partially supported by Grant-in-Aid for Scientific Research (C) 23560663, by the Global COE Program "The Research and Training Center for New Development in Mathematics," and by the Aihara Project, the FIRST program from JSPS, initiated by CSTP.

A MILP formulation

In section 5, we have formulated the optimization problem for design of tensegrity structures, problem (26), and shown that this optimization problem can be reformulated as an MILP problem. This MILP problem has been solved in section 6 by using a commercial MILP solver.

The explicit description of this MILP problem is given as

$$
\begin{aligned}
\min_{\boldsymbol{x},\boldsymbol{y},\boldsymbol{z},\boldsymbol{q}} \quad & \sum_{i\in E} l_i y_i && && \text{(27a)}\\
\text{s.t.} \quad & H\boldsymbol{q} = \boldsymbol{0}, && && \text{(27b)}\\
& -\overline{q}^{\mathrm{s}} x_i \le q_i \le -\underline{q}^{\mathrm{s}} x_i + \overline{q}^{\mathrm{c}}(1-x_i), && \forall i \in E, && \text{(27c)}\\
& \underline{q}^{\mathrm{c}} y_i - \overline{q}^{\mathrm{s}}(1-y_i) \le q_i \le \overline{q}^{\mathrm{c}} y_i, && \forall i \in E, && \text{(27d)}\\
& \sum_{i\in E(v_p)} x_i \le 1, && \forall v_p \in V, && \text{(27e)}\\
& y_i \le \sum_{i'\in E(v_p)} x_{i'}, \quad \forall i \in E(v_p), && \forall v_p \in V, && \text{(27f)}\\
& \sum_{i\in E} x_i \ge \bar{s}, && && \text{(27g)}\\
& x_i + x_{i'} + y_i + y_{i'} \le 1, && \forall (i,i') \in P_{\mathrm{cross}}, && \text{(27h)}\\
& z_j \le \sum_{i\in E_j} x_i, && \forall j \in B, && \text{(27i)}\\
& \frac{1}{|E_j|} \sum_{i\in E_j} x_i \le z_j, && \forall j \in B, && \text{(27j)}\\
& \sum_{j\in B} z_j = \bar{b}, && && \text{(27k)}\\
& \sum_{i\in E} (5x_i - y_i) = \bar{d} + 6, && && \text{(27l)}\\
& \sum_{i\in E(v_p)} y_i \ge 3 \sum_{i\in E(v_p)} x_i, && \forall v_p \in V, && \text{(27m)}\\
& x_i \in \{0,1\}, \quad y_i \in \{0,1\}, && \forall i \in E, && \text{(27n)}\\
& z_j \in \{0,1\}, && \forall j \in B, && \text{(27o)}\\
& x_i + y_i \le 1, && \forall i \in E. && \text{(27p)}
\end{aligned}
$$

Note that constraint (27p) is a valid inequality constraint, because constraints (27c), (27d), and (27n) imply (27p).

References

[1] Bai, Y., de Klerk, E., Pasechnik, D., Sotirov, R.: Exploiting group symmetry in truss topology optimization. *Optimization and Engineering*, **10**, 331–349 (2009),

[2] Baudriller, H., Maurin, B., Cañadas, P., Montcourrier, P., Parmeggiani, A., Bettache, N.: Form-finding of complex tensegrity structures: application to cell cytoskeleton modelling. *Comptes Rendus Mécanique*, **334**, 662–668 (2006)

[3] Bel Hadj Ali, N., Rhode-Barbarigos, L., Pascual Albi, A.A., Smith, I.F.C.: Design optimization and dynamic analysis of a tensegrity-based footbridge. *Engineering Structures*, **32**, 3650–3659 (2010).

[4] Calladine, C.R.: Buckminster Fuller's "tensegrity" structures and Clerk Maxwell's rules for the construction of stiff frames. *International Journal of Solids and Structures*, **14**, 161–172 (1978).

[5] Connelly, R., Back, A.: Mathematics and tensegrity. *American Scientist*, **86**, 142–151 (1998).

[6] Connelly, R., Fowler, P.W., Guest, S.D., Schulze, B., Whiteley, W.J.: When is a symmetric pin-jointed framework isostatic? *International Journal of Solids and Structures*, **46**, 762–773 (2009).

[7] Connelly, R., Terrell, M.: Globally rigid symmetric tensegrities. *Structural Topology*, **21**, 59–77 (1995).

[8] Connelly, R., Whiteley, W.: Second-order rigidity and prestress stability for tensegrity frameworks. *SIAM Journal on Discrete Mathematics*, **6**, 453–491 (1996).

[9] Fowler, P.W., Guest, S.D.: A symmetry extension of Maxwell's rule for rigidity of frames. *International Journal of Solids and Structures*, **37**, 1793–1804 (2000).

[10] Guest, S.D.: The stiffness of prestressed frameworks: a unifying approach. *International Journal of Solids and Structures*, **43**, 842–854 (2006).

[11] Guo, X., Ni, C., Cheng, G., Du, Z.: Some symmetry results for optimal solutions in structural optimization. *Structural and Multidisciplinary Optimization*, to appear.

[12] Gurobi Optimization, Inc.: *Gurobi Optimizer Reference Manual*. `http://www.gurobi.com/` (2010).

[13] Hanaor, A.: Prestressed pin-jointed structures—flexibility analysis and prestress design. *Computers and Structures*, **28**, 757–769 (1988).

[14] Hanaor, A., Liao, M.-K.: Double-layer tensegrity grids: static load response. Part I: analytical study. *Journal of Structural Engineering (ASCE)*, **117**, 1660–1674 (1991).

[15] Heartney, E.: *Kenneth Snelson: Forces Made Visible*. Hard Press Editions, Lenox (2009).

[16] IBM ILOG: *User's Manual for CPLEX*. `http://www.ilog.com/` (2010).

[17] Juan, S.H., Mirats Tur, J.M.: Tensegrity frameworks: static analysis review. *Mechanism and Machine Theory*, **43**, 859–881 (2008).

[18] Kanno, Y.: Topology optimization of tensegrity structures under self-weight loads. *Journal of the Operations Research Society of Japan*, **55**, 125–145 (2012).

[19] Kanno, Y.: Topology optimization of tensegrity structures under compliance constraint: a mixed integer linear programming approach. *Optimization and Engineering*, to appear. Also: METR 2011–39, Department of Mathematical Informatics, University of Tokyo, November 2011 (available at `http://www.keisu.t.u-tokyo.ac.jp/research/techrep/`).

[20] Kanno, Y., Guo, X.: A mixed integer programming for robust truss topology optimization with stress constraints. *International Journal for Numerical Methods in Engineering*, **83**, 1675–1699 (2010).

[21] Kanno, Y., Ohsaki, M., Murota, K., Katoh, N.: Group symmetry in interior-point methods for semidefinite program. *Optimization and Engineering*, **2**, 293–320 (2001).

[22] Li, Y., Feng, X.-Q., Cao, Y.-P., Gao, H.: A Monte Carlo form-finding method for large scale regular and irregular tensegrity structures. *International Journal of Solids and Structures*, **47**, 1888–1898 (2010).

[23] Li, Y., Feng, X.-Q., Cao, Y.-P., Gao, H.: Constructing tensegrity structures from one-bar elementary cells. *Proceedings of the Royal Society A, Mathematical, Physical and Engineering Sciences*, **466**, 45–61 (2010).

[24] Masic, M., Skelton, R.E., Gill, P.E.: Algebraic tensegrity form-finding. *International Journal of Solids and Structures*, **42**, 4833–4858 (2005).

[25] Micheletti, A., Williams, W.O.: A marching procedure for form-finding for tensegrity structures. *Journal of Mechanics of Materials and Structures*, **2**, 857–882 (2007).

[26] Motro, R.: *Tensegrity*. Kogan Page Science, London (2003).

[27] Pellegrino, S.: A class of tensegrity domes. *International Journal of Space Structures*, **7**, 127–142 (1992).

[28] Pellegrino, S., Calladine, C.R.: Matrix analysis of statically and kinematically indeterminate frameworks. *International Journal of Solids and Structures*, **22**, 409–428 (1986).

[29] Rasmussen, M.H., Stolpe, M.: Global optimization of discrete truss topology design problems using a parallel cut-and-branch method. *Computers and Structures*, **86**, 1527–1538 (2008).

[30] Rieffel, J., Valero-Cuevasa, F., Lipson, H.: Automated discovery and optimization of large irregular tensegrity structures. *Computers and Structures*, **87**, 368–379 (2009).

[31] Ross, E., Schulze, B., Whiteley, W.: Finite motions from periodic frameworks with added symmetry. *International Journal of Solids and Structures*, **48**, 1711–1729 (2011).

[32] Rozvany, G.I.N.: On symmetry and non-uniqueness in exact topology optimization. *Structural and Multidisciplinary Optimization*, **43**, 297–317 (2011).

[33] Schulze, B., Whiteley, W.: The orbit rigidity matrix of a symmetric framework. *Discrete and Computational Geometry*, **46**, 561–598 (2011).

[34] Skelton, R., de Oliveira, M.C.: *Tensegrity Systems*. Springer, Dordrecht (2009).

[35] Stolpe, M.: On some fundamental properties of structural topology optimization problems. *Structural and Multidisciplinary Optimization*, **41**, 661–670 (2010).

[36] Stolpe, M., Svanberg, K.: Modelling topology optimization problems as linear mixed 0–1 programs. *International Journal for Numerical Methods in Engineering*, **57**, 723–739 (2003).

[37] Tibert, A.G., Pellegrino, S.: Review of form-finding methods for tensegrity structures. *International Journal of Space Structures*, **18**, 209–223 (2003).

[38] Tran, H.C., Lee, J.: Determination of a unique configuration of free-form tensegrity structures. *Acta Mechanica*, **220**, 331–348 (2011).

[39] Tran, H.C., Lee, J.: Form-finding of tensegrity structures with multiple states of self-stress. *Acta Mechanica*, **222**, 131–147 (2011).

[40] Watada, R., Ohsaki, M., Kanno, Y.: Non-uniqueness and symmetry of optimal topology of a shell for minimum compliance. *Structural and Multidisciplinary Optimization*, **43**, 459–471 (2011).

[41] Xu, X., Luo, Y.: Form-finding of nonregular tensegrities using a genetic algorithm. *Mechanics Research Communications*, **37**, 85–91 (2010).

[42] Zhang, J.Y., Guest, S.D., Ohsaki, M.: Symmetric prismatic tensegrity structures. Part II: symmetry-adapted formulations. *International Journal of Solids and Structures*, **46**, 15–30 (2009).

[43] Zhang, J.Y., Ohsaki, M.: Stability conditions for tensegrity structures. *International Journal of Solids and Structures*, **44**, 3875–3886 (2007).

[44] Zhang, L., Maurin, B., Motro, R.: Form-finding of nonregular tensegrity systems. *Journal of Structural Engineering (ASCE)*, **132**, 1435–1440 (2006).